

NJC

## Accepted Manuscript



This is an *Accepted Manuscript*, which has been through the RSC Publishing peer review process and has been accepted for publication.

*Accepted Manuscripts* are published online shortly after acceptance, which is prior to technical editing, formatting and proof reading. This free service from RSC Publishing allows authors to make their results available to the community, in citable form, before publication of the edited article. This *Accepted Manuscript* will be replaced by the edited and formatted *Advance Article* as soon as this is available.

To cite this manuscript please use its permanent Digital Object Identifier (DOI®), which is identical for all formats of publication.

More information about *Accepted Manuscripts* can be found in the [Information for Authors](#).

Please note that technical editing may introduce minor changes to the text and/or graphics contained in the manuscript submitted by the author(s) which may alter content, and that the standard [Terms & Conditions](#) and the [ethical guidelines](#) that apply to the journal are still applicable. In no event shall the RSC be held responsible for any errors or omissions in these *Accepted Manuscript* manuscripts or any consequences arising from the use of any information contained in them.

Cite this: DOI: 10.1039/c0xx00000x

www.rsc.org/xxxxxx

ARTICLE TYPE

# Novel naphthyridine-based compounds in small molecular non-doped OLEDs: synthesis, properties and their versatile applications for organic light-emitting diodes†

Antonio Fernández-Mato, José M. Quintela\* and Carlos Peinador\*

5 Received (in XXX, XXX) XthXXXXXXXXXX 20XX, Accepted Xth XXXXXXXXXXXX 20XX  
DOI: 10.1039/b000000x

A series of six new n-type conjugated 1,8-naphthyridine oligomers were examined in organic light emitting diodes (OLEDs). The compounds show a high fluorescence in both solution ( $10^{-8}$  M) and the solid state. The naphthyridines have high glass-transition ( $T_g = 65$ - $105$  °C) and decomposition ( $T_d = 380$ - $400$  °C) temperatures, reversible electrochemical reduction, and high electron affinities (2.79-3.00 eV). Systematic variation of the spacer linkage can modulate and fine-tuning their properties. They emit a high blue, green and yellow photoluminescence with 0.70-1.0 quantum yields. Good-performance, single-layer emitter OLEDs with yellow to white-pink emission has also been demonstrated using these materials. White-pink emitter give a performance with a high brightness ( $400$   $\text{cd}\cdot\text{m}^{-2}$  at 4 V), and 0.6  $\text{cd}/\text{A}$ . Yellow emitters give the best performance with maximum brightness of  $250$   $\text{cd}\cdot\text{m}^{-2}$  with a maximum current efficiency of 1.2  $\text{cd}/\text{A}$ . These results demonstrate the potential of this new class of n-type conjugated oligomers as emitters and electron-transport materials for developing high-performance yellow to white-pink OLEDs.

## Introduction

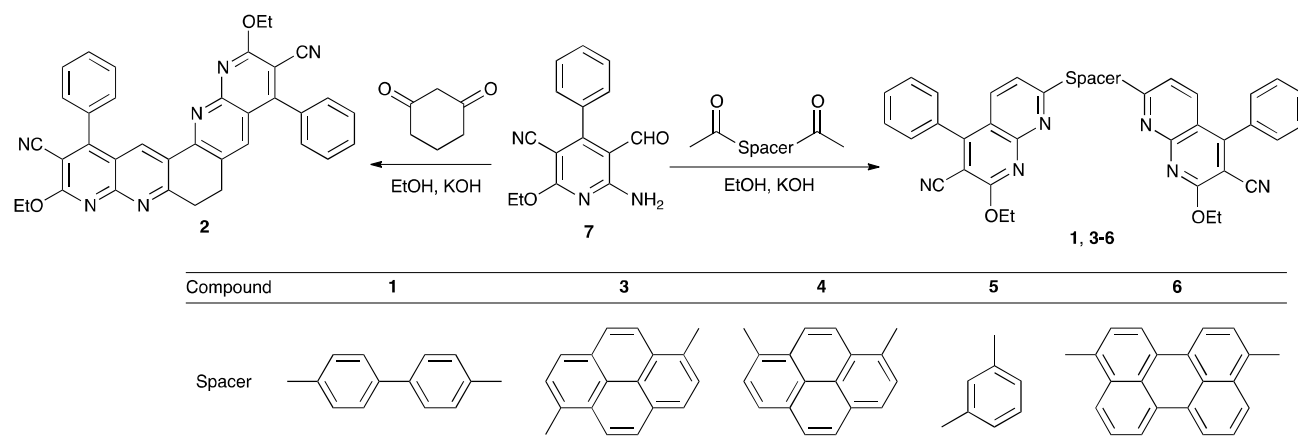
20 Since the discovery of organic light-emitting diodes (OLEDs) at Eastman Kodak Company by Tang and Van Slyke using small-molecules (sm-OLEDs),<sup>1</sup> there has been substantial effort aimed at developing highly efficient electroluminescent (EL) materials, and considerable progress has been made on both small-molecule- and polymer-based OLEDs.<sup>2</sup> In particular, small organic conjugated molecules with a built-in donor-acceptor architecture have attracted increasing attention as active materials in organic optoelectronic devices such as OLEDs,<sup>3,4</sup> organic solar cells (OSCs),<sup>5</sup> field effect transistors (OFETs),<sup>6</sup> solid-state lasers,<sup>7</sup> and the possibility of innovative applications to new classes of displays<sup>8</sup> and light sources.<sup>9</sup> They provide notable advantages, however, the strong intermolecular interaction of common conjugated organic molecules makes it extremely difficult to dissolve them and even then they tend to form crystalline domains in the film state.<sup>10</sup> Therefore, it is of significant importance for future OLEDs applications to design and subsequently synthesize amorphous molecules in high purity that exhibit high fluorescence quantum efficiency and are highly soluble.

40 Small-molecule-based OLEDs are considered more valuable than the polymer counterparts because of the difficulty in controlling the film thickness with polymers and the possibility of dissolution of the first layer during the coating of the second layer by spin-coating techniques,<sup>11</sup> although intensive work has been made to overcome this limitation.<sup>12</sup> Several criteria need to be fulfilled for

developing the materials used in single-layer OLEDs: (1) high emission quantum yield; (2) good and balanced electron and hole mobilities; (3) high glass-transition temperature; (4) matched highest occupied molecular orbital (HOMO) and lowest unoccupied molecular orbital (LUMO) energy levels with the energy levels of the anodes and cathodes. The first three criteria have to be tackled by appropriate molecular design and the fourth criterion can be assisted by surface/interface modification/engineering of the electrodes.

55 To be useful as an electron transporter in an OLED, a given material must be chemically and thermally stable and have an electron-deficient  $\pi$  system. Although a large number of small molecules, oligomers, and polymers have been investigated for applications in OLEDs, the vast majority of the structure-property studies have been devoted to organic materials having dominant p-type (electron donor, hole transport) properties.<sup>13</sup> A number of different organic molecules have been used as electron transporters, including oxadiazoles, triazoles, phenanthrolines, quinolines, quinoxalines, 1,5-naphthyridines, anthrazolines, 1,8-naphthalimides, pyrazinoquinoxalines, and thienopyrazine derivatives.<sup>14</sup> The efficiency of small organic molecules as emitters in OLEDs, particularly for display purpose, requires highly efficient light-emitting materials with enhanced electron injection and transport properties.<sup>15</sup>

70 Herein, we report the synthesis, full characterization, and investigation of the theoretical modelling, photophysics, electrochemistry, EL, and device fabrication/characterization of new types of 1,8-naphthyridine (napy)-based molecules, including 4,4'-di[(6'-cyano-7'-ethoxy-5'-phenyl)-1,8-



**Scheme 1** Synthesis of oligonaphthyridines **1-6**.

naphthyridin-2'-yl][1,1-biphenyl] (**1**), 3,11-dicyano-2,10-diethoxy-4,12-diphenyl-6,7-dihydrobenzo[1,2-*b*:3,4-*b'*]1,8-binaphthyridine (**2**), 1,6-di[(6'-cyano-7'-ethoxy-5'-phenyl)-1,8-naphthyridin-2'-yl]pyrene (**3**), 1,8-di[(6'-cyano-7'-ethoxy-5'-phenyl)-1,8-naphthyridin-2'-yl]pyrene (**4**), 1,3-di[(6'-cyano-7'-ethoxy-5'-phenyl)-1,8-naphthyridin-2'-yl]benzene (**5**), and 3,10-di[(6'-cyano-7'-ethoxy-5'-phenyl)-1,8-naphthyridin-2'-yl]perylene (**6**). As shown in Scheme 1, this new class of n-type conjugated oligomers has a common bis(napy) core and various aromatic substituents as conjugated spacers. This molecular design facilitates retention of n-type characteristics due to the bis-naphthyridine core, while allowing variation of the electronic structure (HOMO/LUMO levels) and physical properties by means of the aromatic-anchored spacer group. Experimental results show that the compounds were synthesized by Friedländer route and have good solubility in organic solvents, excellent thermal properties with high glass transition temperatures ( $T_g$ ), high thermal decomposition, high quantum yield and good film properties. The potential of napy in ELs has not been vastly explored, and the emission maximum of naphthyridines can be conveniently tuned by structural modifications.<sup>9</sup>

## Experimental

### Material and methods

Di-1,8-naphthyridines (**1-5**) were prepared from 2-amino-5-cyano-6-ethoxy-3-formyl-4-phenylpyridine and the corresponding diketone (4,4'-diacetyl biphenyl, 1,2-cyclohexanedione, 1,3-diacetylbenzene, 1,6-diacetylpyrene, 1,8-diacetylpyrene) according to a procedure by Quintela, Peinador et al.<sup>16</sup> All the reagents were purchased from Sigma-Aldrich and were used without further purification. Merck 60 F254 foils were used for thin layer chromatography, and Merck 60 (230-400 mesh) silica gel was used for flash chromatography. Proton and carbon nuclear magnetic resonance spectra were recorded on a Bruker Avance-300 or Bruker Avance-500 equipped with a dual cryoprobe for <sup>1</sup>H and <sup>13</sup>C, using the deuterated solvent as lock and the residual protonated solvent as internal standard. Mass spectrometry experiments were carried out in a LC-Q-q-TOF Applied Biosystems QSTAR Elite spectrometer for low- and high-resolution ESI. TGA were recorded on a SDT 2960TA instruments, DSC were recorded Q 100TA instruments and UV

data were recorded on a Jasco V-650 Spectrophotometer, fluorescence spectra were recorded on Perkin-Elmer LS45 fluorescence spectrometer. Cyclic voltammetry experiments were made using Autolab equipment with a PGSTAT 20 potentiostat at 25°C. A platinum electrode was used as the working electrode and a platinum rod as the counter electrode. A silver wire was used as a pseudo reference electrode and calibrated with ferrocene as internal standard. All the potentials reported in this work are referenced to the classical Fc<sup>+</sup>-Fc standard couple. All experiments were carried out in acetonitrile under dry argon and with tetrabutylammonium perchlorate as supporting electrolyte.

### Synthesis

#### Synthesis of 3,10-diacetylperylene (**8**).

To a solution of perylene (1.0 g, 5.95 mmol) in CS<sub>2</sub> (16 mL) was added anhydrous AlCl<sub>3</sub> (17.98 mmol). The darkness solution was cooled to 4 °C and acetyl chloride (13.16 mmol) was added with stirring during 10 minutes under argon atmosphere. The solution was raised to room temperature and after 8 hours, water-ice mixture (100 mL) was poured. The green precipitate was filtered and purified by flash chromatography on silica gel using CH<sub>2</sub>Cl<sub>2</sub> as eluent to give **8** (0.79 g, 40%). <sup>1</sup>H NMR (CDCl<sub>3</sub>, 300 MHz): 2.75 (s, 6H, 2CH<sub>3</sub>); 7.65 (d, *J* = 7.8 Hz, 2H); 7.96 (d, *J* = 8.4 Hz, 2H); 8.23 (d, *J* = 8.4 Hz, 2H); 8.29 (d, *J* = 8.0 Hz, 2H); 8.79 (dd, *J* = 8.4 Hz, *J* = 8.0 Hz, 2H). MS (FAB<sup>+</sup>, *m/z*): 337.12 (M+H)<sup>+</sup>. Anal. Calcd. C<sub>24</sub>H<sub>16</sub>O<sub>2</sub>: C, 85.69; H, 4.79. Found. C, 85.77; H, 4.84.

#### Synthesis of 3,10-bis[(6'-cyano-7'-ethoxy-5'-phenyl)-1,8-naphthyridin-2'-yl]perylene (**6**).

A solution of 2-amino-5-cyano-6-ethoxy-3-formyl-4-phenylpyridine (**7**)<sup>17</sup> (0.27 g, 1.0 mmol), 3,10-diacetylperylene (**8**) (0.168 g, 0.50 mmol) and a catalytic amount of ethanolic potassium hydroxide (10 %) in ethanol (15 mL) was refluxed until all starting material had disappeared as checked by TLC (12 h). After cooling, the precipitate was collected by filtration and purified by flash chromatography on silica gel using CH<sub>2</sub>Cl<sub>2</sub> as eluent to give **6** (0.23 g, 60%). <sup>1</sup>H NMR (CDCl<sub>3</sub>, 300 MHz): 1.59 (t, *J* = 7.1 Hz, 6H, 2CH<sub>3</sub>); 4.85 (c, *J* = 7.1 Hz, 4H, 2OCH<sub>2</sub>); 7.53-7.68 (m, 12H); 7.70 (d, *J* = 8.4 Hz, 2H); 7.85 (d, *J* = 7.8 Hz, 2H); 8.07 (d, *J* = 8.4 Hz, 2H); 8.12 (d, *J* = 8.4 Hz, 2H); 8.33 (d, *J* = 8.4 Hz, 2H); 8.36 (d, *J* = 8.4 Hz, 2H). <sup>13</sup>C NMR (CDCl<sub>3</sub>, 75 MHz): 14.4 (CH<sub>3</sub>); 64.3 (OCH<sub>2</sub>); 99.0; 114.3 (CN); 116.4; 119.7; 120.3;

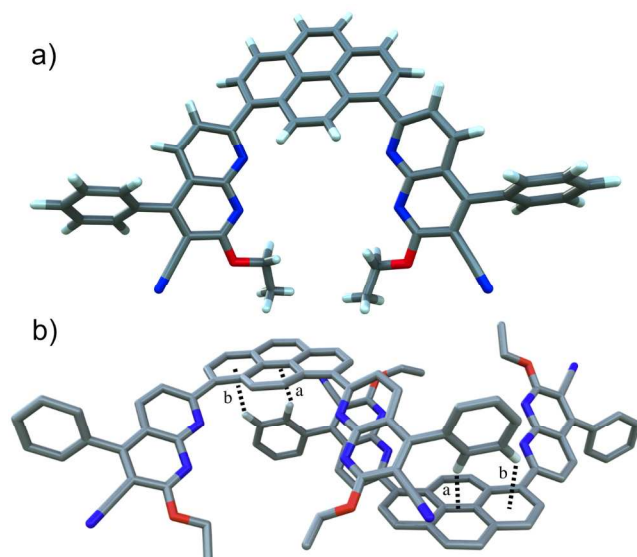


**Fig. 1** a) Crystal structure of compound **4**. b) Crystal packing of **4** showing [C—H... $\pi$ ] interactions ([H...centroid] and, [C...centroid] distances and [C—H...centroid] angle): a 2.68 Å, 3.60 Å, 154°; b 2.99 Å, 3.81 Å, 139°.

123.1; 123.1; 127.4; 129.1; 130.3; 131.3; 132.2; 133.1; 136.6; 137.1; 156.0; 158.4; 162.8; 164.6. MS (FAB<sup>+</sup>, *m/z*): 799.2 (M+H)<sup>+</sup>. Anal. Calcd. C<sub>54</sub>H<sub>34</sub>N<sub>6</sub>O<sub>2</sub>: C, 81.19; H, 4.29; N, 10.52. Found C, 81.57; H, 4.64; N, 10.11.

### 5 Device Fabrication and Testing

The layers were spin-coated onto pre-patterned ITO glass plates (prior to deposition, the ITO-coated glass substrates were extensively cleaned, using chemical and UV-ozone methods) and the layers were subsequently annealed at 200 °C on a hotplate for 30 min. Before spin-coating the solutions were filtered over a 0.20  $\mu$ m PTFE filter. The thicknesses of the spin-coated films were determined using an Ambios XP1 profilometer. Current density and luminance versus voltage were measured using a Keithley 2400 source meter and a photodiode coupled to a Keithley 6485 picoammeter using a Minolta LS100 to calibrate the photocurrent. An Avantes luminance spectrometer was used to measure the electroluminescence spectrum. EQE values were obtained assuming a Lambertian emission. The fabrication process of the devices was as follows: Firstly, PEDOT was spin-coated on a precleaned and UV/ozone treated ITO substrate and dried. Secondly, the materials for the hole-transporting layer (HTL) were dissolved in chlorobenzene and spin-coated on top of the PEDOT layer or evaporated.

### Crystallographic Data

CCDC-796293 contains the supplementary crystallographic data for compound **4**.<sup>18</sup> These data can be obtained free of charge from the Cambridge Crystallographic Data Centre via [www.ccdc.cam.ac.uk/data\\_request/cif](http://www.ccdc.cam.ac.uk/data_request/cif). The structure was solved by direct methods and refined with the full-matrix least-squares procedure (SHELX-97) against *F*<sup>2</sup>. The X-ray diffraction data were collected on a Bruker X8 ApexII diffractometer. Non-solvent hydrogen atoms were placed in idealized positions with  $U_{eg}(H) = 1.2U_{eg}(C)$  and were allowed to ride on their parent atoms. Solvent hydrogen atoms were placed in idealized positions with  $U_{eg}(H) =$

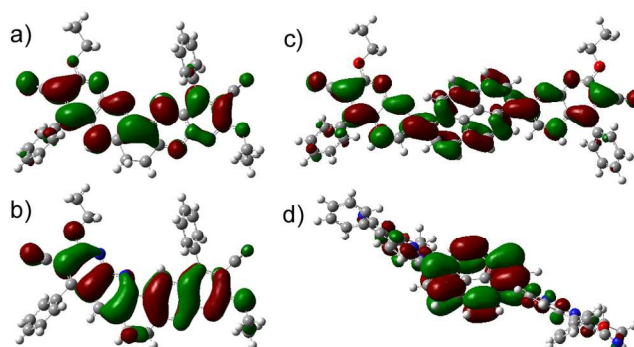


**Fig. 2** LUMO and HOMO levels calculated of **2** (figures a and b, respectively) and **3** (figures c and d).

1.5 $U_{eg}(C)$  and were allowed to ride on their parent atoms.

## Results and discussion

### Synthesis and Characterization

Scheme 1 shows the synthesis of the oligonaphthyridines (**1-6**). Di-1,8-naphthyridines (**1-5**) were already prepared and characterized from 2-amino-5-cyano-6-ethoxy-3-formyl-4-phenylpyridine and the corresponding diketone. Compound **6** was prepared from **7** and 3,10-diacetylperylene (**8**) under base-catalyzed Friedländer giving the desired product in 60% yield. Compound (**6**) was isolated by filtration and the material eluted through silica-gel column via flash chromatography. The chemical structures of **6** were confirmed by <sup>1</sup>H-NMR, <sup>13</sup>C-NMR, mass spectrometry and elemental analysis as described in the experimental section. X-ray analysis of **4** was carried out to establish the structure of the bis-napy compounds. As shown in Figure 1a, there is not coplanarity between the linker pyrene and the end napy groups. The dihedral angle between the linker unit and the naphthyridine moiety is 123°, this twist in the structure results in the reduction of the  $\pi$  conjugation between the linker and the napy end moieties. The asymmetric unit of the triclinic P-1 unit cell has one molecule of **4** and one molecule of deuterated nitromethane (both in general positions). The molecule of **4** has approximate mirror symmetry, with the pseudo mirror plane lying across the pyrene ring, as can be seen in Figure 1a. The molecular packing exhibits intermolecular C-H... $\pi$  edge-to-face interactions between phenyl moiety (C-H21 and C-H8) ring and pyrene ring (Figure 1b). Intermolecular  $\pi$ - $\pi$  electronic interaction between aromatic rings is not observed, where this features may reduce the excimer formation in the solid state as already observed in ladder-type structures.<sup>19</sup>

To have better understanding of the properties of (**1-6**), calculations on its electronic ground state were carried out using a B3LYP density functional theory<sup>20</sup> with a 6-31G(d) basis in the Gaussian 03 program.<sup>21</sup> The optimized geometry and electron-density distribution of the highest occupied molecular orbital (HOMO) and lowest unoccupied molecular orbital (LUMO) are shown in Figure 2 where illustrates calculated spatial distributions of the energy levels of the designed molecule **3** and naphthyridine-containing perturbed ring **2**. The spatial distributions of the LUMO and HOMO levels are partially separated in **3**, where the HOMO lies at pyrene moiety and LUMO at napy and pyrene moiety, which indicates that the

[View Online](#)**Table 1** Physical properties of compounds **1-6**.

	$T_m/T_g/T_d$ [°C] <sup>a</sup>	$\lambda_{\text{abs}}$ [nm]	$\lambda_{\text{abs}}$ [nm]	$\lambda_{\text{abs}}$ [nm]	$\lambda_{\text{em}}$ [nm]	$\lambda_{\text{em}} (\Phi_F)$	$\lambda_{\text{em}} (\Phi_F)$	$E_{\text{red}}^{\text{onset}}$ [V] <sup>c</sup>	HOMO/LUMO [eV] <sup>f</sup>
		CH <sub>3</sub> CN <sup>b</sup>	CH <sub>2</sub> Cl <sub>2</sub> <sup>b</sup>	film <sup>b</sup>	CH <sub>3</sub> CN <sup>c</sup>	[nm, %] CH <sub>2</sub> Cl <sub>2</sub> <sup>c</sup>	[nm, %] film <sup>d</sup>		
<b>1</b>	385/99/401	371, 420	333, 384	387	470	450(100)	443 (15)	-1.65	5.9/2.85
<b>2</b>	340/101/390	378, 420	378, 398	396	450	440(100)	479 (14)	-1.6	6.0/2.9
<b>3</b>	313/105/380	370, 428	328, 418	430	530	530(100)	495 (11)	-1.7	5.50/2.80
<b>4</b>	323/98/388	391, 411	372, 416	420	485	480(98)	500 (11)	-1.65	5.55/2.85
<b>5</b>	340/95/398	358, 372	353, 369	n.d. <sup>f</sup>	490	495(87)	n.d. <sup>g</sup>	-1.71	6.0/2.79
<b>6</b>	350/65/381	430	314, 433	n.d. <sup>f</sup>	545	585(85)	n.d. <sup>g</sup>	-1.5	5.5/3.0

<sup>a</sup> The heating and cooling rates were 15 K/min;  $T_m$ : melting point;  $T_g$ : glass-transition temperature;  $T_d$ : decomposition temperature.

<sup>b</sup>  $\lambda_{\text{abs}}$ : absorption maximum.

<sup>c</sup>  $\lambda_{\text{em}}$ : emission maximum;  $\Phi_F$ : fluorescence quantum yield measured by calibrating against rhodamine B ( $\Phi_F = 0.65$ ) in ethanol as standard.

<sup>d</sup>  $\lambda_{\text{em}}$ : emission maximum;  $\Phi_F$ : fluorescence quantum yield were measured using an integrated sphere.

<sup>e</sup> Measured in CH<sub>3</sub>CN. All the potentials are reported as peak potentials, which are relative to ferrocene (used as the internal standard in each experiment). Ferrocene oxidation potential was calibrated to be +0.3V versus silver wire used as a pseudoreference electrode.

<sup>f</sup> The HOMO and LUMO energies were determined from cyclic voltammetry and the absorption onset.

<sup>g</sup> Not determined.

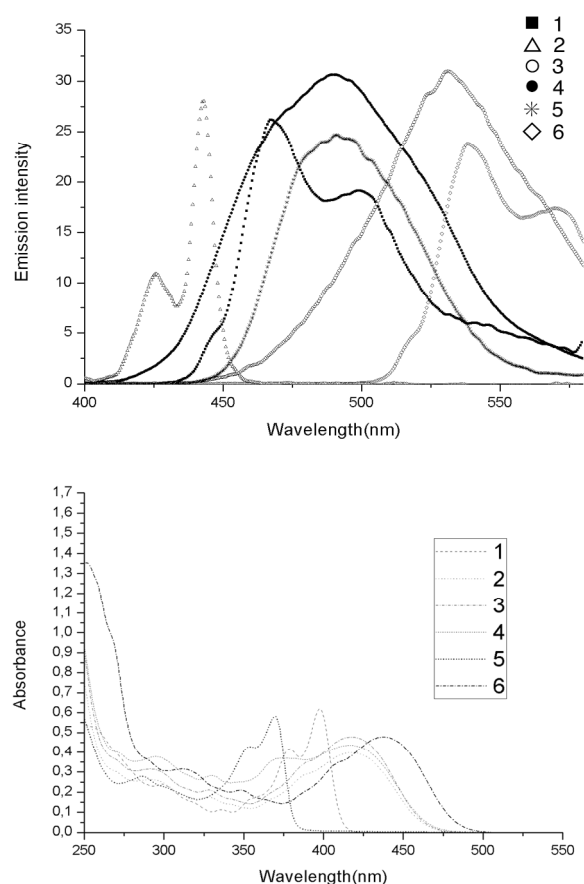


**Fig. 3** Emissionspectra of **1-6** recorded in nitromethane ( $10^{-5}$  M) at 25 °C (top) and absorption (bottom).

HOMO/LUMO transition becomes a typical charge-transfer (CT) transition, while the distribution of the HOMO and LUMO levels

of **2** is slightly segregated compared with that of **3**. This is also preferable for efficient hole- and electron-transfer properties and the prevention of back transfer. Besides, from the optimized geometry of **3** it can be seen that the linker are twisted, which makes the molecular structure nonplanar, thus facilitating the formation of an amorphous film (see Supplementary data) and reducing the intermolecular  $\pi$ - $\pi$  stacking and/or interaction.

All the di-napy compounds (**1-6**) are readily soluble in common organic solvents, such chloroform, dichloromethane, tetrahydrofuran or nitromethane. The good solubility of the compounds is desirable for the fabrication of solution-processed, low-cost, large area OLEDs. The thermal properties were determined by thermo-gravimetric analysis (TGA) and differential scanning calorimetry (DSC) measurements. As shown in Table 1, the oligonaphthyridines hold high  $T_g$  values in the range of 65-105 °C. None of the compounds exhibited a melting point when heated to 300 °C and cooled to room temperature by DSC. TGA measurements showed that the compounds are thermally stable up to 300 °C with a  $T_d$  in the range of 380-400 °C in nitrogen. The excellent thermal stability with high  $T_g$  and  $T_d$  values should improve the morphological stability of the film and reduce the possibility of phase separation upon heating.<sup>22</sup>

### Photophysical Properties

The photophysical properties of the oligonaphthyridine derivatives were measured using UV-vis absorption and photoluminescence (PL) spectroscopy, and the data are summarized in Table 1 and Figure 3. The PL studies on films were performed to examine the emission in the condensed phase. The films were made by spin casting of their solutions in dichlorobenzene onto the quartz plates. In the UV-visible spectra, the absorption bands observed around 350-418 nm can be attributed to  $\pi$ - $\pi^*$  transitions of the conjugated aromatic segments. PL spectra indicate that **3** and **4** are red-shifted by about 40 and 80 nm in CH<sub>2</sub>Cl<sub>2</sub>, respectively,

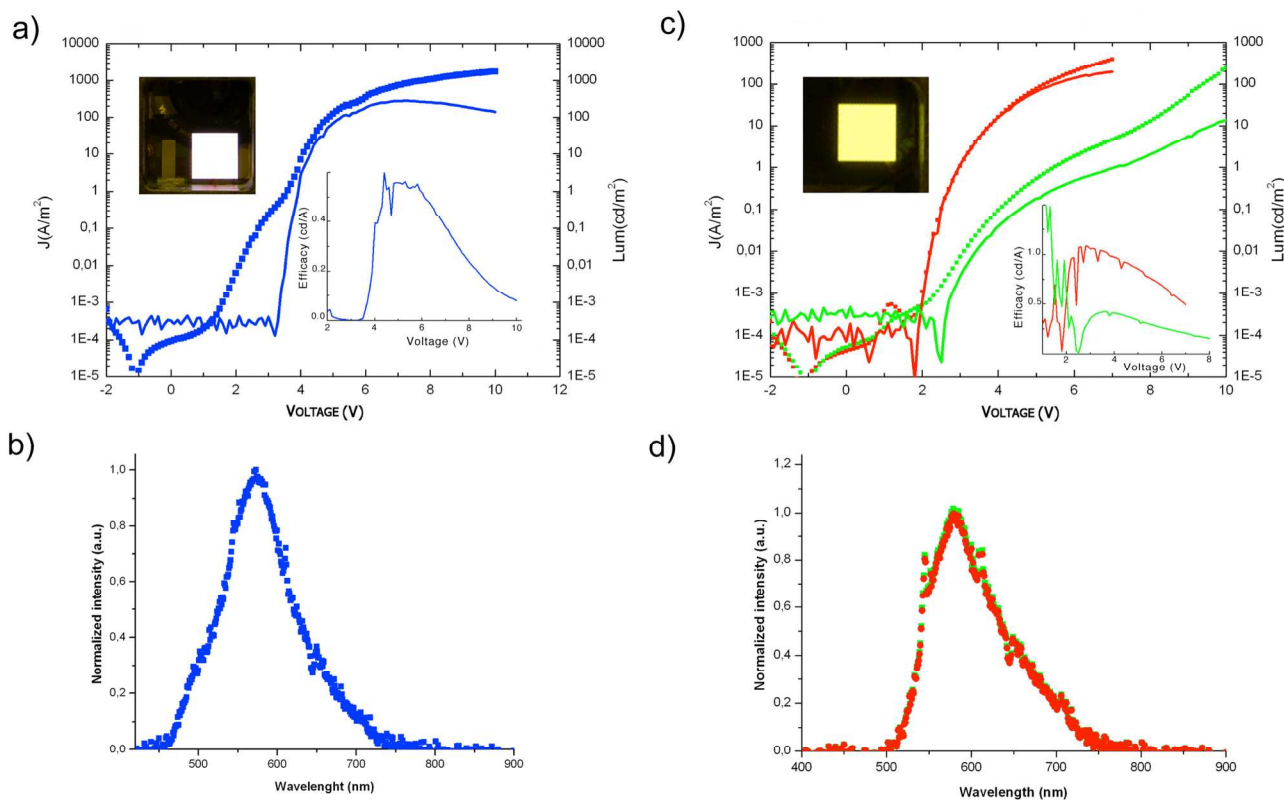


**Fig. 4** a) Current density and luminance versus voltage of OLED A (the inset shows the normalized efficacy versus voltage and the operation image of device A). b) EL spectrum of the device A. c) Current density and luminance versus voltage of OLEDs B (green) and C (red). The inset shows the operation image of devices B and C. d) Normalized EL spectra of the devices B (green) and C (red).

compared with **2** as a result of the extension of aromatic moiety. Compounds (**1-6**) exhibit very high emission intensities at concentrations as low as  $10^{-8}$  M. The effect of an increase in conjugation is clearly revealed in the emission maxima, which vary from ca. 450 to 580 nm (blue to yellow). Thus, the emission properties can be modulated by appropriate structural modifications.

All compounds are emissive in the blue, green and yellow region, both in the solution and in the film state (Table 1). The trend of the  $\lambda_{em}$  values among the different compounds is parallel with that of  $\lambda_{abs}$  values: (1) compounds with a more delocalization linker shown larger  $\lambda_{abs}$  y  $\lambda_{em}$ . The fluorescence quantum yields of all the compounds in dichloromethane are in the 0.7-1.0 range and were measured by calibrating against rhodamine B in ethanol as standard ( $\Phi_F = 0.65$ ). On the basis of the long-wavelength onset of the absorption band for the samples, the bandgaps of (**1-6**) were estimated to be 2.5-3.3 eV decreasing with increasing the size of linker.

The electron affinity (EA) or LUMO levels of the oligonaphthyridines (**1-6**) were determined by voltammetry cyclic (CV), and these data, together with the absorption spectra, were then taken to obtain the HOMO energy levels. Clearly, the theoretical DFT results for the designed molecules agree well with the experimental ones, which imply that the HOMO and LUMO can be controlled by the incorporation of linker size. The bandgaps estimated from the DFT calculations are similar (2.3–3.5 eV) than those obtained from the measurements, and the trend

is identical.

### Electrochemistry

Cyclic voltammetry (CV) experiments were conducted to investigate the electrochemical properties of the compounds. Both the oxidation and reduction cycles of the samples were measured in acetonitrile, using tetrabutylammonium hexafluorophosphate as the electrolyte and ferrocene as internal reference, and the  $E_{FOC}$  was calibrated to be 0.3 V versus a silver wire that was used as a pseudo reference electrode. All of these compounds exhibit one reversible, one-electron redox wave due the process of reduction and the LUMO or EA was calculated using the equation:  $LUMO = -(4.5 + E_{red})$  eV. The onset potential of the reduction process ranges from  $-1.5$  to  $-1.71$  V. By using the reduction potentials and bandgap in absorption spectra, the LUMO levels for the samples (**1-6**) were calculated and found to be between  $-2.79$  and  $-3.0$  eV, whereas the values for the highest occupied molecular orbital (HOMO) levels for (**1-6**) lay between  $-6.0$  to  $-5.5$  eV (Table 1).

### Electroluminescence

Because of the high PL quantum efficiencies of compounds (**1-6**), the use of the materials as emitters in OLED devices was also explored. Films were fabricated by either vacuum deposition or spin coating. All films were formed with quality amorphous film with fairly smooth surface and devices consisting of **2** or **3** as emitting layers could be fabricated and characterized. Three

View Online

device with ITO/PEDOT8000/TCTA (Tris[4-(carbazol-4-yl)phenyl]amine): **3** (spin-coated)/BCP (2,9-dimethyl-4,7-diphenyl-1,10-phenanthroline)/BCP:Cs<sub>2</sub>CO<sub>3</sub>/Al (A), ITO/PEDOT8000/PVK Poly(N,N'-diphenyl-N,N'-bis(4-hexylphenyl)-[1,1'-biphenyl]-4,4'-diamine) (30 nm)/**2** (vacuum deposition) (35 nm)/LiF/Al (B) and ITO/PEDOT8000/p-TPD/TCTA(20 nm)/**2** (vacuum deposition) (35 nm)/LiF/Al (C) were fabricated. The devices architecture was chosen according the good energy level matches between layers. BCP serves as a good hole and exciton blocker, The performances of the devices with different hosts are illustrated in Figure 4. As can be seen, devices A, B and C for compounds 2 and 3 exhibited a quite low turn-on voltage, bright luminance, and respectable external quantum efficiency. It can be seen that all devices fabricated by using the napy moieties have a low turn-on voltage (4-6 V). The turn on voltage of A was 3.5 V with a brightness of 1cd·m<sup>-2</sup> and maximum brightness of 400 cd·m<sup>-2</sup> at 4 V. The maximum current efficiency is 0.6 cd/A. B device containing evaporated film of 2, with a turn-on voltage of 7 V (with a brightness of 1 cd·m<sup>-2</sup>) and maximum brightness of 15 cd·m<sup>-2</sup> with a maximum current efficiency is 1.5 cd/A. C device containing evaporated film of 2, shown turn-on voltage of 3 V (with a brightness of 1 cd·m<sup>-2</sup>) and maximum brightness of 250 cd·m<sup>-2</sup> with a maximum current efficiency of 1.2 cd/A. The EL spectra of the devices A-C, shown in Figure 4, differ significantly from the PL of 3 and 2. The device A exhibits a white-pink EL with the spectrum covering almost the whole visible range with band centred at 590 nm. The blue and green part of both EL and PL spectra are originated from the same radiation-decay process of singlet excitons. The emission in the red region to 600-700 nm appears only in the EL spectrum of 3.

The spectra reveal white-pink emissions according to the CIE chromaticity diagram (0.1706, 0.319). The devices B and C exhibit yellow emission according CIE diagram (B 0.5204, 0.4893; C 0.5089, 0.4075). The white-pink and yellow emissions in devices A, B, and C are produced only by electric excitation. According previous results obtained in the references, the emission in the red and yellow regions in our devices may arise from the singlet electromer, where similar disparity in the EL and PL spectra has also been reported previously and the radioactive decay of electromer or electroplex was usually responsible for the additional emission in EL.<sup>23</sup> The electromer could be regarded as an excited state of a pair of naphthyridine molecules with opposite charges under electrical excitation, in which one carried an excess electron while the other carried a hole. Note that most of the electromers reported in the bibliography were formed at relatively high electric fields, but here were formed at 4-5 eV. The white-pink and yellow emission in devices A and B may result of fluorescence and electromer emission. The devices does not change the colour emission with voltage applied.

## Conclusions

A series of new 1,8-naphthyridine (napy)-based molecules has been synthesized from a simple and efficient route and characterized. A simple and systematic variation of the spacer linkage can modulate and fine-tuning their properties. These compounds show a high fluorescence in both solution (10<sup>-8</sup> M) and the solid state. Relative good quantum efficiencies have been

achieved. Using different conjugated spacers and linking topologies allowed tuning of the HOMO and LUMO energies. The experimental results indicate that (1-6) have a potential for the use in yellow and white-pink OLEDs with a facile preparation methods. Further study is in progress in order to optimize the devices A-C by modifying the layers to enhance the performance.

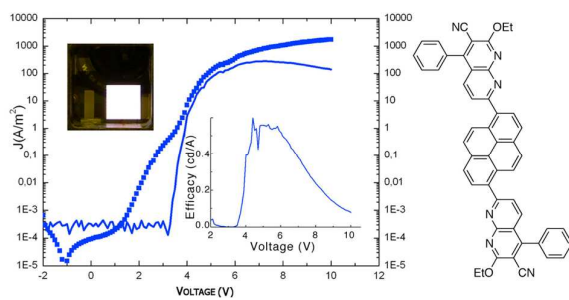
## Acknowledgment

This research was supported by Ministerio Ciencia e Innovación and FEDER (CTQ2010-16484/BQU). We thank Henk Bolink and Sonsoles García (ICMOL, Valencia, Spain) for device fabrications.

## Notes and references

- Departamento de Química Fundamental, Universidade da Coruña, Facultad de Ciencias, A Zapateira, s/n, 15008, La Coruña, Spain. Fax: +34 981167065; E-mail: carlos.peinador@udc.es jose.maria.quintela@udc.es
- † Electronic Supplementary Information (ESI) available: Powder X-ray diffraction patterns of compound 3 in film and cyclic voltammetry data. See DOI: 10.1039/b000000x/
- C. W.Tang and S. A. Van Slyke, *Appl. Phys. Lett.*, 1987, **51**, 913.
- For recent reviews, see: (a) S. C. Lo and P. L. Burn, *Chem. Rev.*, 2007, **107**, 1097; (b) J. Shinar and R. Shinar, *J. Phys. D: Appl. Phys.*, 2008, **41**, 13301; (c) F. So and J. Shi, *Opt. Sci. Eng.*, 2008, **133**, 351; (d) T. K. S. Wong, in *Handbook of Organic Electronics and Photonics* H. S. Nalga, Ed. American Scientific Publishers: Stevenson Ranch, CA, 2008 Vol 2, 413.
- (a) J. H. Burroughes, D. D. C. Bradley, A. R. Brown, R. N. Marks, K. Mackay, R. H. Friend, P. L. Burns and A. B. Homes, *Nature*, 1990, **347**, 539; (b) A. P. Kulkarni, X. Kong and S. A. Jeneckhe, *Adv. Funct. Mater.*, 2006, **16**, 1057; (c) H. Yan, P. Lee, N. R. Armstrong, A. Gram, G. A. Evmenenko, P. Dutta and T. J. Marks, *J. Am. Chem. Soc.*, 2005, **127**, 3172; (d) G. Hughes and M. R. Bryce, *J. Mater. Chem.*, 2005, **15**, 94; (e) C. T. Chen, *Chem. Mater.*, 2004, **16**, 4389; (f) Y. Shirota, *J. Mater. Chem.*, 2000, **10**, 1; (g) R. E. Martin and F. Diederich, *Angew. Chem., Int. Ed.*, 1999, **38**, 1350; (h) G. Liu, X.-Y. Miao, W.-L. Deng, W. Yang, Y. Cao and J. Roncali, *Macromol. Rapid Commun.*, 2009, **30**, 1484.
- (a) C. J. Tonzola, A. P. Kulkarni, A. P. Gifford, W. Kaminsky and S. A. Jeneckhe, *Adv. Funct. Mater.*, 2007, **17**, 863; (b) M.-Y. Lai, C.-H. Chen, W.-S. Huang, J. T. Lin, T.-H. Ke, L.-Y. Chen, M.-H. Tsai and C.-C. Wu, *Angew. Chem., Int. Ed.*, 2008, **47**, 581; (c) A. Kraft, A. C. Grimsdale and A. B. Colmes, *Angew. Chem. Int. Ed.*, 1998, **37**, 402; (d) S. R. Forrest, *Nature*, 2004, **428**, 911; (e) J. Brown, R. Kwong, Y.-J. Tung, V. Adamovich, M. Weaver and M. Hack, *J. Soc. Inf. Disp.*, 2004, **12**, 329; (f) R. Q. Yang, Y. H. Xu, X. D. Dang, T. D. Nguyen, Y. Cao and G. C. Bazan, *J. Am. Chem. Soc.*, 2008, **130**, 3282; (g) J. M. Hancock, A. P. Gifford, C. J. Tonzola and S. A. Jeneckhe, *J. Phys. Chem. C*, 2007, **111**, 6875.
- (a) M. T. Lloyd, J. E. Anthony and G. G. Malliaras, *Mater. Today*, 2007, **10**, 36; (b) J. Roncali, P. Leriche and A. Cravino, *Adv. Mater.*, 2007, **19**, 2045; (c) M. Jorgensen and F. C. Krebs, *J. Org. Chem.*, 2005, **70**, 6004.
- (a) H. Sirringhaus, *Proc. IEEE*, 2009, **97**, 1570; (b) C. D. Dimitrakopoulos and P. R. L. Malenfant, *Adv. Mater.*, 2002, **14**, 99; (c) S. Allard, M. Forster, B. Souharce, H. Thiem and U. Scherf, *Angew. Chem., Int. Ed.*, 2008, **47**, 4070.
- (a) J. Huang, Q. Liu, J. H. Zou, X.-H. Zhu, A.-Y. Li, J.-W. Li, S. Wu, J. B. Peng, Y. Cao, R. Xiu, D. D. C. Bradley and J. Roncali, *Adv. Funct. Mater.*, 2009, **19**, 2978; (b) I. D. W. Samuel and G. A. Turnbull, *Chem. Rev.*, 2007, **107**, 1272; (c) R. D. Xia, W. Y. Lai, P. A. Levermore, W. Huang and D. D. C. Bradley, *Adv. Funct. Mater.*,

- 2009, **19**, 2844; (d) W. Y. Lai, R. D. Xia, Q. Y. He, P. A. Levermore, W. Huang and D. D. C. Bradley, *Adv. Funct. Mater.*, 2009, **21**, 355.
- 8 (a) P. Andersson, D. Nilsson, P. O Svensson, M. X. Chen, A. Malmstrom, T. Remonen and M. Bergen, *Adv. Mater.* 2002, **14**, 1460. (b) J. Kido, M. Kimura and K. Nagai, *Science*, 1995, **267**, 1332.
- 9 (a) Y. Chen, J. Au, P. Kazlas, A. Ritenour, H. Gates and M. McCreary, *Nature*, 2003, **423**, 136; (b) R. A. Hayes and B. J. Feenstra, *Nature*, 2003, **425**, 383; (c) S. Park, J. E. Kwon, S. H. Kim, J. Seo, K. Cheng, S.-Y. Park, D.-J. Jang, B. M. Medina, J. Gierschner and S. Y. Park, *J. Am. Chem. Soc.*, 2009, **131**, 14043.
- 10 (a) P. Strohriegel and J. V. Grazulevicius, *Adv. Mater.*, 2002, **14**, 1439; (b) S. Wang, W. J. Oldham Jr., R. A. Hudack and G. C. Bazan, *J. Am. Chem. Soc.*, 2000, **122**, 5695; (c) M. D. Joswick, I. H. Campbell, N. N. Barashkov, J. P. Ferraris, *J. Appl. Phys.*, 1996, **80**, 2883.
- 11 H. Yersin and W. J. Finkensteller, in *Highly Efficient OLEDs with Phosphorescent Materials* H. Yersin, Ed. Wiley-VCH: Weinheim, Germany 2008, Ch. 1.
- 12 (a) C. D. Müller, A. Falcou, N. Reckefuss, M. Rojahn, V. Wiederhirn, P. Rudati, H. Frohne, O. Nuyken, H. Becker and K. Meerholz, *Nature*, 2003, **421**, 829; (b) M. Gather, A. Köhnen, A. Falcou, H. Becker and K. Meerholz, *Adv. Funct. Mater.*, 2007, **17**, 191; (c) M. C. Gather, F. Ventsch and K. Meerholz, *Adv. Mater.*, 2008, **20**, 1966; (d) A. Köhnen, N. Riegel, J. H.-W. M. Kremer, H. Lademann, M. C. Müller and K. Meerholz, *Adv. Mater.*, 2009, **21**, 879; (e) F. Ventsch, M. C. Gather and, K. Meerholz, *Organic Electronics*, 2010, **11**, 57; (f) A. Charas, H. Alves, José M. G. Martinho, L. Alcácer, O. Fenwick, F. Cacialli and J. Morgado, *Synth. Met.* 2008, **158**, 643; (g) A. Charas, H. Alves, L. Alcácer and J. Morgado, *Appl. Phys. Lett.*, 2006, **89**, 143519.
- 13 (a) A. P. Kulkarni, X. Kong and S. A. Jeneckhe, *Adv. Funct. Mater.*, 2006, **16**, 1057; (b) H. Yan, P. Lee, N. R. Armstrong, A. Gram, G. A. Evemenenko, P. Dutta and P. J. Marks, *J. Am. Chem. Soc.*, 2005, **127**, 3172; (c) P. T. Furuta, L. Deng, S. Garon, M. E. Thompson and J. M. Frechet, *J. Am. Chem. Soc.*, 2004, **126**, 15388; (d) A. P. Kulkarni, Y. Zhu and S. A. Jeneckhe, *Macromolecules*, 2005, **38**, 1553; (e) G. Hughes and M. R. Bryce, *J. Mat. Chem.*, 2005, **15**, 94; (f) C. Chi and G. Wegner, *Macromol. Rapid Commun.*, 2005, **26**, 1532; (g) *Electronic Materials: The Oligomer Approach*, K. Mullen, G. Wegner, Eds. Wiley-VCH: Weinheim, Germany, 1998.
- 14 (a) A. P. Kulkarni, X. Kong and S. A. Jeneckhe, *Macromolecules*, 2006, **39**, 8699; (b) Y. Zhu, R. D. Champion and S. A. Jeneckhe, *Macromolecules*, 2006, **39**, 8712; (c) S. P. Economopoulos, A. K. Andreopoulos, V. G. Gregoriou and J. K. Kallitsis, *Chem. Mater.*, 2005, **17**, 1063; (d) S.-H. Liao, J.-R. Shiu, S.-W. Liu, S.-J. Yeh, Y.-H. Chen, C.-T. Chen, T. J. Chow and C.-I. Wu, *J. Am. Chem. Soc.*, 2009, **131**, 763; (e) C. Adachi, R. C. Kwong, P. Djurovich, V. Adamovich, M. A. Baldo, M. E. Thompson and S. R. Forrest, *Appl. Phys. Lett.*, 2001, **79**, 2082; (f) C. Adachi, M. Baldo, S. R. Forrest and M. E. Thompson, *Appl. Phys. Lett.*, 2000, **77**, 904; (g) Y. Li, Y. Liu, W. Bu, D. Lu, Y. Wu and Y. Wang, *Chem. Mater.*, 2000, **12**, 2672; (h) D. Kolosov, V. Adamovich, P. Djurovich, M. E. Thompson and C. Adachi, *J. Am. Chem. Soc.*, 2002, **124**, 9945.
- 15 (a) A. P. Kulkarni, C. J. Tonzol, A. Babel and S. A. Jeneckhe, *Chem. Mater.*, 2004, **16**, 783; (b) J. Huang, C. Li, Y. J. Xia, X. H. Zhu, J. B. Peng and Y. Cao, *J. Org. Chem.*, 2007, **72**, 8580; (c) J. Huang, X. F. Qiao, Y. J. Xia, X. H. Zhu, D. G. Ma, Y. Cao and J. Roncali, *Adv. Mater.*, 2008, **20**, 4172; (d) A. C. A. Chen, S. W. Culligan, Y.-H. Geng, S.-H. Chen, K. P. K. Klubek, M. Vaeth and C. W. Tang, *Adv. Mater.*, 2004, **16**, 783.
- 16 A. Fernández-Mato, G. Blanco, J. M. Quintela and C. Peinador, *Tetrahedron*, 2008, **64**, 3446.
- 17 J. M. Quintela and J. L. Soto, *An. Quim.*, 1984, **80C**, 268.
- 18 Crystal data for **4**: C<sub>51</sub>27D<sub>8</sub>N<sub>7.5</sub>O<sub>5</sub>, *M* = 840.91, Triclinic, *a* = 9.2902(2) Å, *b* = 13.6836(3) Å, *c* = 16.0690(3) Å, *α* = 85.5210(10)°, *β* = 80.3570(10)°, *γ* = 88.5340(10)°, *V* = 2007.57(7) Å<sup>3</sup>, *T* = 100(2) K, space group *P*-1, *Z* = 2, *μ*(MoK $\alpha$ ) = 0.263 mm<sup>-1</sup>, 25214 reflections measured, 9545 independent reflections (*R*<sub>int</sub> = 0.0336). The final *R*<sub>i</sub> values were 0.0535 (*I* > 2 $\sigma$ (*I*)). The final *wR*(*F*<sup>2</sup>) values were 0.1447 (*I* > 2 $\sigma$ (*I*)). The final *R*<sub>i</sub> values were 0.0763 (all data). The final *wR*(*F*<sup>2</sup>) values were 0.1669 (all data). The goodness of fit on *F*<sup>2</sup> was 1.036.
- 19 (a) K. T. Wong, T. C. Chao, L. C. Chi, Y. Y. Chu, A. Balaiah, S. F. Chiu, Y. H. Liu and Y. Wang, *Org. Lett.*, 2006, **8**, 5033; (b) K. T. Wong, L. Chi, S. C. Huang, Y. L. Liao, Y. H. Liu and Y. Wang, *Org. Lett.*, 2006, **8**, 5029.
- 20 (a) A. D. Becke, *Phys. Rev.*, A, 1998, **38**, 3098; (b) C. Lee, W. T. Yang and R. G. Parr, *Phys. Rev. B*, 1988, **37**, 785.
- 21 Gaussian-03 (Rev. Co2 and D01).
- 22 I. Vedija and J. P. Dodelet, *Chem. Mater.*, 2001, **13**, 1739; (b) G. S. Liou, S. H. Hsiao, W. C. Chen and H. J. Yen, *Macromolecules*, 2006, **39**, 6036.
- 23 R. Adhikari, L. Duan, L. Hou, Y. Qiu, D. Neckers and B. Shah, *Chem. Mater.*, 2009, **21**, 4638.

[View Online](#)

A series of new 1,8-naphthyridine-based molecules has been synthesized, the experimental results indicate that these compounds have a potential for the use in yellow and white-pink OLEDs with a facile preparation methods.